

Contents

Chapter	Subject	Author	Page
	List of Tables		vii
	List of Figures		xi
	The RATE Group		xxiv
	Prologue	John D. Morris	xxv
	Acknowledgments		xxix
1	Introduction	Larry Vardiman	1
2	Young Helium Diffusion Age of Zircons Supports Accelerated Nuclear Decay	D. Russell Humphreys	25
3	Radiohalos in Granites: Evidence for Accelerated Nuclear Decay	Andrew A. Snelling	101
4	Fission Tracks in Zircons: Evidence for Abundant Nuclear Decay	Andrew A. Snelling	209
5	Do Radioisotope Clocks Need Repair? Testing the Assumptions of Isochron Dating Using K-Ar, Rb-Sr, Sm-Nd, and Pb-Pb Isotopes	Steven A. Austin	325

6	Isochron Discordances and the Role of Inheritance and Mixing of Radioisotopes in the Mantle and Crust	Andrew A. Snelling	393
7	Accelerated Decay: Theoretical Considerations	Eugene F. Chaffin	525
8	¹⁴ C Evidence for a Recent Global Flood and a Young Earth	John R. Baumgardner	587
9	Statistical Determination of Genre in Biblical Hebrew: Evidence for an Historical Reading of Genesis 1:1–2:3	Steven W. Boyd	631
10	Summary of Evidence for a Young Earth from the RATE Project	Larry Vardiman Steven A. Austin John R. Baumgardner Steven W. Boyd Eugene F. Chaffin Donald B. DeYoung D. Russell Humphreys Andrew A. Snelling	735
	Index		773

List of Tables

Table	Title	Page
Introduction		
1	Results of high priority experiments	8
2	Results of additional significant experiments	9
3	Results of low priority experiments	11
Young Helium Diffusion Age of Zircons		
Supports Accelerated Nuclear Decay		
1	Helium retentions in zircons from the Jemez granodiorite	29
2	Latest (2003) Jemez zircon diffusion data for about 1200 50–75 μm length zircon crystals from borehole GT-2 at a depth of 1490 m	45
3	New Creation model	51
4	Uniformitarian model	54
5	Helium diffusion age of zircons	56
6	Billion-year uniformitarian retentions versus observed retentions	57
A1	U-Pb analyses of three zircons from the Jemez granodiorite	76
B1	Diffusion of He from biotite sample BT-1B	78
B2	Diffusion of He from biotite sample GT-2	80
C1	Diffusion data for zircon sample YK-511	82
Radiohalos in Granites: Evidence for Accelerated Nuclear Decay		
1	Radiohalos recorded in Precambrian (pre-Flood) granitic rocks	115
2	Radiohalos recorded in Paleozoic-Mesozoic (Flood) granitic rocks	116

Table	Title	Page
3	Radiohalos recorded in Tertiary (post-Flood) granitic rocks	118
4	Radiohalos recorded in regional metamorphic rocks	188

Fission Tracks in Zircons: Evidence for Abundant Nuclear Decay

1	Details of the samples obtained for this study, including locations, geological age designations and previously published age determinations	218
2	Results of the zircon fission track dating of twelve tuff samples from the Grand Canyon-Colorado Plateau region	238
3	The mineral composition of the $2-4\ \mu\text{m}$ fraction of Muav and Tapeats tuff samples MT-3 and TT-1 respectively determined by XRD analyses	265
4	The U-Th-Pb radioisotope analyses and ages of abraded zircon grains from Muav tuff sample MT-3 and Tapeats tuff sample TT-1	271

Do Radioisotope Clocks Need Repair? Testing the Assumptions of Isochron Dating Using K-Ar, Rb-Sr, Sm-Nd, and Pb-Pb Isotopes

1	Major-element oxide and selected trace element analyses of the Beartooth andesitic amphibolite from the southeastern Beartooth Mountains, northwest Wyoming	346
2	Whole-rock, major-element oxide and selected trace element analyses of eleven samples from the Bass Rapids sill, Grand Canyon, northern Arizona	351
3	K-Ar data for the whole rock and selected minerals from the Beartooth andesitic amphibolite, sample BT-1, northwestern Wyoming	353
4	Whole-rock and mineral Rb-Sr, Sm-Nd and Pb-Pb radioisotopic data for the Beartooth andesitic amphibolite, sample BT-1, northwestern Wyoming	353

Table	Title	Page
5	K-Ar data for whole rocks from the Bass Rapids diabase sill, Grand Canyon, northern Arizona	357
6	Whole-rock Rb-Sr, Sm-Nd and Pb-Pb radioisotopic data for the Bass Rapids diabase sill, Grand Canyon, northern Arizona	360
7	Mineral Rb-Sr, Sm-Nd and Pb-Pb radioisotopic data for diabase sample DI-13 from the Bass Rapids sill, Grand Canyon, northern Arizona	362
8	Mineral Rb-Sr, Sm-Nd and Pb-Pb radioisotopic data for diabase sample DI-15 from the Bass Rapids sill, Grand Canyon, northern Arizona	362
9	Magnetite and ilmenite Rb-Sr, Sm-Nd and Pb-Pb radioisotopic data for the Bass Rapids diabase sill, Grand Canyon, northern Arizona	363
Isochron Discordances and the Role of Inheritance and Mixing of Radioisotopes in the Mantle and Crust		
1	K-Ar model and isochron "ages" obtained for the targeted rock units	411
2	K-Ar, Rb-Sr, Sm-Nd and Pb-Pb isochron "ages" for the targeted rock units	414
3	Sr-Nd-Pb isotope geochemistry data obtained for the targeted rock units	422
Accelerated Decay: Theoretical Considerations		
1	Results of calculations for Oklo samples	539
2	Sensitivity of various forbidden β -decays to changes in decay energy	566
3	Data on the ratios R for each sample	570

Table	Title	Page
¹⁴C Evidence for a Recent Global Flood and a Young Earth		
1	AMS measurements on samples conventionally deemed older than 100 ka	596
2	Results of AMS ¹⁴ C analysis of ten RATE coal samples	605
3	Detailed AMS ¹⁴ C measurements for ten RATE coal samples in pMC	608
4	AMS ¹⁴ C results for six African diamonds	611
5	AMS ¹⁴ C result for six alluvial diamonds from Namibia	612
6	AMS ¹⁴ C results for the twelve diamonds with the laboratory's standard background correction applied	614
 Statistical Determination of Genre in Biblical Hebrew: Evidence for an Historical Reading of Genesis 1:1–2:3		
1	Classification table (by passage)	668
B1	Finite verb counts for narrative: Torah	698
B2	Finite verb counts for narrative: Former Prophets	699
B3	Finite verb counts for narrative: Latter Prophets	699
B4	Finite verb counts for narrative: Writings	700
B5	Finite verb counts for poetry: Torah	700
B6	Finite verb counts for poetry: Former Prophets	701
B7	Finite verb counts for poetry: Latter Prophets	701
B8	Finite verb counts for poetry: Writings	702
C1	Parameter estimation section	703
C2	Model summary section	703
D1	Retrospections on the past	705
D2	Origins of names and sayings	705
D3	Historical footnotes	706
D4	Sources cited	707
D5	Chronological reference points	708
D6	Function of genealogies	710
D7	Commemorative days and feasts	711
D8	Temporal continuity	712

List of Figures

Figure	Title	Page
Young Helium Diffusion Age of Zircons		
Supports Accelerated Nuclear Decay		
1	Zircons from the Jemez granodiorite	26
2	Nuclear decay makes He within zircons	27
3	Drilling rig at Fenton Hill, New Mexico	28
4	He atom moving through a crystal	32
5	Typical Arrhenius plot	35
6	Increasing number of defects slides the defect line upward	36
7	Interpretations of Russian zircon data compared with Nevada zircon data	37
8	Observed diffusion coefficients in zircons	40
9	Observed diffusion coefficients in two types of mica	41
10	Scanning electron microscope photo of a zircon leached in HF	42
11	Scanning electron microscope photo of a zircon from size-selected sample 2003	43
12	Spherical approximation of the zircon-biotite system	47
13	The 2003 zircon data line up very well with the Creation model, and resoundingly reject the uniformitarian model	55
14	New retention point confirms Gentry's retention data	59
15	Lines of Figure 13 redrawn in accordance with the 2003 data	60
16	Different temperatures cannot rescue the uniformitarian model	62
17	Closure and re-opening of a zircon	64
18	Two hourglasses representing two methods of dating zircons	66
19	Particle motion in curved space	71

Figure	Title	Page
Radiohalos in Granites: Evidence for Accelerated Nuclear Decay		
1	Sunburst effect of α -damage trails	103
2	Schematic drawing of (a) a ^{238}U halo, and (b) a ^{232}Th halo, with radii proportional to the ranges of α -particles in air	104
3	Composite schematic drawing of (a) a ^{218}Po halo, (b) a ^{238}U halo, (c) a ^{214}Po halo, and (d) a ^{210}Po halo, with radii proportional to the ranges of α -particles in air	106
4	Some typical examples of the different radiohalos found in granitic rocks in this study	119
5	Plot of the conventional age (in millions of years) versus the total number of radiohalos per slide (per sample) for each granitic pluton	122
6	Plot of the conventional age (in millions of years) versus the number of Po radiohalos per slide (per sample) for each granitic pluton	123
7	Time sequence of diagrams to show schematically the formation of ^{238}U and ^{210}Po radiohalos concurrently as a result of hydrothermal fluid flow along biotite cleavage planes	134
8	Cross-section of the margin of a magma chamber	154
9	^{218}Po and ^{214}Po radiohalos centered along cracks in biotite flakes and continuous overlapping overexposed ^{210}Po radiohalos	162
10	The effects of hydrothermal fluids on biotite—chloritization and fluid inclusions	172
Fission Tracks in Zircons: Evidence for Abundant Nuclear Decay		
1	Correlation of the Cambrian Tonto Group showing facies changes in the western Grand Canyon	217

Figure	Title	Page
2	Map of Utah showing the location of the three Brushy Basin Member stratigraphic sections sampled	220
3	Schematic measured stratigraphic section showing the lithologies and unit numbers in the Morrison Formation, Notom, Utah	221
4	Schematic measured stratigraphic section showing the lithologies and unit numbers in the Morrison Formation in the Brushy Basin, west of Blanding, Utah	222
5	Schematic measured stratigraphic section showing the lithologies in the Brushy Basin Member of the Morrison Formation at Montezuma Creek, Utah	224
6	Map showing the distribution of the Peach Spring Tuff	225
7	Map of the Kingman area, Arizona, showing the local extent of the Peach Springs Tuff	226
8	Schematic measured section through the Peach Spring Tuff along Interstate-40 west of Kingman, Arizona	228
9	Some of the zircon grains recovered from six of the tuff samples in this study	234
10	The spontaneous fission tracks in the polished and etched surfaces of some of the mounted zircon grains in five of the tuff samples in this study	236
11	Basic construction of a normal radial plot	240
12	Simplified structure of a normal radial plot and an arc sin radial plot	241
13	Radial plots and histograms of the individual zircon grain fission track ages in the early Middle Cambrian tuff samples from the western Grand Canyon	243
14	Radial plots and histograms of the individual zircon grain fission track ages in the Upper Jurassic Morrison Formation tuff samples from south-eastern Utah	244
15	Radial plots and histograms of the individual zircon grain fission track ages in the Miocene Peach Springs Tuff samples from south-eastern California and western Arizona	246

Figure	Title	Page
16	The XRD patterns for the oriented and glycolated <math><2-4\mu\text{m}</math> fractions of Muav and Tapeats tuff samples MT-3 and TT-1 respectively	265
17	Proportion of illite layers in mixed-layer illite/smectite versus depth and temperature from wells in the Gulf of Mexico coast region	267
18	Zircon grains from Muav tuff sample MT-3 selected for U-Th-Pb radioisotope analyses	269
19	Zircon grains from Tapeats tuff sample TT-1 selected for U-Th-Pb radioisotope analyses	270
20	Concordia plots of the U-Pb radioisotope data obtained for zircon grains from Muav tuff sample MT-3	272
21	$^{206}\text{Pb}/^{204}\text{Pb}$ versus $^{207}\text{Pb}/^{204}\text{Pb}$ isochrons fitted to the Pb radioisotope data obtained from the six zircon grains from Muav tuff sample MT-3	273
22	Concordia plot of the U-Pb radioisotope data obtained from three zircon grains from Tapeats tuff sample TT-1	274
23	$^{206}\text{Pb}/^{204}\text{Pb}$ versus $^{207}\text{Pb}/^{204}\text{Pb}$ isochrons fitted to the Pb radioisotope data obtained from the six zircon grains from Tapeats tuff sample TT-1	275
24	Schematic illustration of the process of formation of a fission track in a crystalline insulating solid	288
25	A comparison of specimen ages determined by fission track analyses with those from historical or other radiometric sources	289
26	Diagram to show the dating range for fission track analysis of different kinds of geological material according to U content	291
27	Schematic illustration of the population method of fission track analysis	292
28	Schematic illustration of the difference between 4π (spherical) and 2π (hemi-spherical) geometry in track formation	294

Figure	Title	Page
29	Schematic illustration of the external detector method of fission track analysis	295
30	Fading of fission tracks in apatite and sphene	306
31	Closing temperatures for retention of fission tracks for minerals cooling at different rates	308

Do Radioisotope Clocks Need Repair? Testing the Assumptions of Isochron Dating Using K-Ar, Rb-Sr, Sm-Nd, and Pb-Pb Isotopes

1	Location map showing the distribution of Precambrian rocks in the northern Rocky Mountain region	330
2	Location of the Bass Rapids diabase sill in Grand Canyon, northern Arizona	332
3	Composite Rb-Sr whole-rock isochron from the Long Lake granitic complex in the southeastern Beartooth Mountains of northwestern Wyoming	334
4	The original Rb-Sr whole-rock isochron plot for the Bass Rapids diabase sill	337
5	Diagrammatic section through the Bass Rapids sill showing the 6 m thick granophyre capping above the 85 m thick diabase body of the sill	343
6	Rb-Sr mineral isochron for the Beartooth andesitic amphibolite	354
7	Sm-Nd mineral isochron for the Beartooth andesitic amphibolite	354
8	Pb-Pb mineral isochron for the Beartooth andesitic amphibolite	355
9	^{40}K versus $^{40}\text{Ar}^*$ in the Bass Rapids diabase sill	358
10	$^{40}\text{K}/^{36}\text{Ar}$ versus $^{40}\text{Ar}/^{36}\text{Ar}$ in the Bass Rapids diabase sill	359
11	Rb-Sr whole-rock isochron for the Bass Rapids diabase sill	361
12	Rb-Sr mineral isochron for diabase samples DI-13 from the Bass Rapids diabase sill	364

Figure	Title	Page
13	Rb-Sr mineral isochron for diabase sample DI-15 from the Bass Rapids diabase sill	364
14	Rb-Sr magnetite mineral isochron for the Bass Rapids diabase sill	365
15	$^{147}\text{Sm}/^{144}\text{Nd}$ versus $^{143}\text{Nd}/^{144}\text{Nd}$ diagram for all eleven whole-rock samples of the Bass Rapids diabase sill	366
16	$^{147}\text{Sm}/^{144}\text{Nd}$ versus $^{143}\text{Nd}/^{144}\text{Nd}$ diagram for six mineral fractions from diabase sample DI-13 (plus the whole rock) from the Bass Rapids diabase sill	367
17	$^{147}\text{Sm}/^{144}\text{Nd}$ versus $^{143}\text{Nd}/^{144}\text{Nd}$ diagram for eight mineral fractions from diabase sample DI-15 (plus the whole rock) from the Bass Rapids diabase sill	368
18	Sm-Nd magnetite mineral isochron for the Bass Rapids diabase sill	369
19	$^{206}\text{Pb}/^{204}\text{Pb}$ versus $^{207}\text{Pb}/^{204}\text{Pb}$ diagram for the Bass Rapids diabase sill, using all eleven whole-rock samples in the isochron and age calculations	370
20	$^{206}\text{Pb}/^{204}\text{Pb}$ versus $^{207}\text{Pb}/^{204}\text{Pb}$ diagram for six mineral fractions from diabase sample DI-13 (plus the whole rock) from the Bass Rapids diabase sill	371
21	$^{206}\text{Pb}/^{204}\text{Pb}$ versus $^{207}\text{Pb}/^{204}\text{Pb}$ diagram for nine mineral fractions from diabase sample DI-15 (plus the whole rock) from the Bass Rapids diabase sill	372
22	$^{206}\text{Pb}/^{204}\text{Pb}$ versus $^{207}\text{Pb}/^{204}\text{Pb}$ diagram for six magnetite mineral fractions from the Bass Rapids diabase sill	373
23	Isochron age versus mode of decay for the four radioisotope systems within Bass Rapids diabase sill	384

Isochron Discordances and the Role of Inheritance and Mixing of Radioisotopes in the Mantle and Crust

1	$^{87}\text{Rb}/^{86}\text{Sr}$ versus $^{87}\text{Sr}/^{86}\text{Sr}$ isochron diagram for the Brahma amphibolites in Grand Canyon	416
---	---	-----

Figure	Title	Page
2	$^{147}\text{Sm}/^{144}\text{Nd}$ versus $^{143}\text{Nd}/^{144}\text{Nd}$ isochron diagram for the Brahma amphibolites in Grand Canyon	417
3	$^{206}\text{Pb}/^{204}\text{Pb}$ versus $^{207}\text{Pb}/^{204}\text{Pb}$ isochron diagram for the Brahma amphibolites in Grand Canyon	418
4	$^{87}\text{Rb}/^{86}\text{Sr}$ versus $^{87}\text{Sr}/^{86}\text{Sr}$ isochron diagram for the Elves Chasm Granodiorite in Grand Canyon	419
5	$^{147}\text{Sm}/^{144}\text{Nd}$ versus $^{143}\text{Nd}/^{144}\text{Nd}$ isochron diagram for the Elves Chasm Granodiorite in Grand Canyon	420
6	$^{206}\text{Pb}/^{207}\text{Pb}$ versus $^{207}\text{Pb}/^{204}\text{Pb}$ isochron diagram for the Elves Chasm Granodiorite in Grand Canyon	421
7	$^{87}\text{Sr}/^{86}\text{Sr}$ versus $^{143}\text{Nd}/^{144}\text{Nd}$ isotope correlation diagram with the whole-rock isotope data from the rock units in this study plotted	423
8	$^{206}\text{Pb}/^{204}\text{Pb}$ versus $^{87}\text{Sr}/^{86}\text{Sr}$ isotope correlation diagram with the whole-rock isotope data from the rock units in this study plotted	424
9	$^{206}\text{Pb}/^{204}\text{Pb}$ versus $^{143}\text{Nd}/^{144}\text{Nd}$ isotope correlation diagram with the whole-rock isotope data from the rock units in this study plotted	425
10	$^{206}\text{Pb}/^{204}\text{Pb}$ versus $^{207}\text{Pb}/^{204}\text{Pb}$ isotope correlation diagram with the whole-rock isotope data from the rock units in this study plotted	426
11	Isochron ages for the Cardenas Basalt, Grand Canyon, plotted against the present half-lives of the parent radioisotopes	433
12	Isochron ages for the Brahma amphibolites, Grand Canyon, plotted against the present half-lives of the parent radioisotopes	433
13	Composite plot of isochron age versus atomic weight for four radioisotope pairs and four Precambrian formations in Grand Canyon	434

Figure	Title	Page
14	Plots of $^{87}\text{Sr}/^{86}\text{Sr}$ and $^{143}\text{Nd}/^{144}\text{Nd}$ versus $^{206}\text{Pb}/^{204}\text{Pb}$ for the recent Ngauruhoe andesites, New Zealand, showing calculated bulk mixing curves	437
15	Dynamic petrogenetic model for andesite magma genesis beneath the Kermadec-Taupo Volcanic Arc subduction system	438
16	$^{87}\text{Sr}/^{86}\text{Sr}$ versus $^{143}\text{Nd}/^{144}\text{Nd}$ isotope correlation diagram with the whole-rock isotope data from selected rock units in this study plotted	440
17	$^{206}\text{Pb}/^{204}\text{Pb}$ versus $^{87}\text{Sr}/^{86}\text{Sr}$ isotope correlation diagram with the whole-rock isotope data from selected rock units in this study plotted	441
18	$^{206}\text{Pb}/^{204}\text{Pb}$ versus $^{143}\text{Nd}/^{144}\text{Nd}$ isotope correlation diagram with the whole-rock isotope data from selected rock units in this study plotted	442
19	$^{206}\text{Pb}/^{204}\text{Pb}$ versus $^{207}\text{Pb}/^{204}\text{Pb}$ isotope correlation diagram with the whole-rock isotope data from selected rock units in this study plotted	443
20	Diagrammatic section through the Bass Rapids sill showing the granophyre "capping" on the diabase, the contact hornfels, the location of samples, and selected whole-rock geochemical and isotope data	445
21	The measured type section of the Cardenas Basalt in Basalt Canyon, eastern Grand Canyon, showing the location of samples and selected whole-rock geochemical and isotope data	447
22	^{40}K versus $^{40}\text{Ar}^*$ isochron diagram for the Bass Rapids sill (diabase and granophyre) and its contact hornfels in Grand Canyon	449
23	$^{87}\text{Rb}/^{86}\text{Sr}$ versus $^{87}\text{Sr}/^{86}\text{Sr}$ isochron diagram for the Bass Rapids sill (diabase and granophyre) and its contact hornfels in Grand Canyon	450

Figure	Title	Page
24	$^{147}\text{Sm}/^{144}\text{Nd}$ versus $^{143}\text{Nd}/^{144}\text{Nd}$ isochron diagram for the Bass Rapids sill (diabase and granophyre) and its contact hornfels in Grand Canyon	451
25	$^{206}\text{Pb}/^{204}\text{Pb}$ versus $^{207}\text{Pb}/^{204}\text{Pb}$ isochron diagram for the Bass Rapids sill (diabase and granophyre) and its contact hornfels in Grand Canyon	452
26	Location and deposits of the Tongariro Volcanic Center, Taupo Volcanic Zone, North Island, New Zealand	466
27	Map of the northwestern slopes of Mt. Ngauruhoe showing the lava flows of 1949 and 1954, the 1975 avalanche deposits, and the location of samples	468
28	Generalized geologic map of the Uinkaret Plateau in the western Grand Canyon region, showing the distribution of basaltic rocks	470
29	Generalized geologic block diagram showing most of the strata sequence and topographic form below the north rim of Grand Canyon	471
30	Location map for the Somerset Dam layered mafic intrusion near Brisbane on Australia's east coast	474
31	Detailed geologic map of the Somerset Dam layered mafic intrusion, southeast Queensland, Australia	475
32	Stratigraphic column for the exposed portion of the Somerset Dam layered mafic intrusion showing its inferred cyclic units, rock densities, and modal compositions	476
33	Location of the Cardenas Basalt and the related Middle Proterozoic named diabase sills and dikes in Grand Canyon	478
34	Outcrop areas of the Middle Proterozoic Apache Group, Troy Quartzite, and associated basalts and diabase sills in central and southern Arizona	487
35	Schematic stratigraphic column of the Apache Group, Troy Quartzite, and associated basalts and diabase sills in central Arizona	489

Figure	Title	Page
36	Simplified geologic map of Paleoproterozoic (Lower Proterozoic) rocks in the Upper and Middle Granite Gorges, Grand Canyon	498
37	Location maps, showing the Beartooth Mountains of Montana and Wyoming and the Long Lake-Beartooth Pass area on U.S. Highway 212	505
38	Simplified geologic map of an area adjacent to, and southeast of, Long Lake and U.S. Highway 212, southern Beartooth Mountains, Wyoming	506
 Accelerated Decay: Theoretical Considerations		
1	The square-well potential with Coulomb barrier	527
2	Sudden change in the number of nodes (zero crossings). The harmonic oscillator wavefunction for well depths of 58 MeV and 54 MeV	529
3	The decay constant versus well depth for the harmonic oscillator interior potential	530
4	The real part of the Coulombic wavefunction outside the Coulomb barrier	531
5	The exponentially diffuse boundary potential and the corresponding wavefunction	531
6	Equilibrium levels of fluid flowing out of buckets through valves that are opened to the same setting	534
7	The percentage $^{234}\text{U}/^{238}\text{U}$ as a function of time, assuming that $^{234}\text{U}/^{238}\text{U}$ begins at 100%	536
8	The percentage $^{234}\text{U}/^{238}\text{U}$ as a function of time, assuming that it begins at 100%	537
9	The position of a pendulum bob, confined to move in a single vertical plane, can be completely specified by a single linear coordinate	542
10	Three closed curves on the surface of a doughnut (torus) illustrate inequivalent and equivalent closed paths	543

Figure	Title	Page
11	The ordinary vibration modes of closed strings and the winding modes	544
12	Considering each point (x, y, z) as equivalent to its reflection $(-x, y, z)$ leads to the quotient space	549
13	A cross-section through a six-dimensional Calabi-Yau shape, generated with <i>Mathematica</i>	550
14	The double β -decay scheme of ^{130}Te	568
15	The ratio R of (radiogenic $^{82}\text{Kr}/^{82}\text{Se}$) divided by $(^{40}\text{Ar}^*/^{40}\text{K})$ versus time	571

^{14}C Evidence for a Recent Global Flood and a Young Earth

1	Layout of the Vienna Environmental Research Accelerator, typical of modern AMS facilities	592
2	Uniformitarian age as a function of $^{14}\text{C}/\text{C}$ ratio, in percent modern carbon	594
3	Distribution of ^{14}C values for non-biogenic Precambrian samples and biologic Phanerozoic samples	595
4	Histogram representation of AMS ^{14}C analysis of ten coal samples undertaken by the RATE ^{14}C research project	606
5	Photo of three diamonds from the Orapa mine, Botswana from the set analyzed in this study	611

Statistical Determination of Genre in Biblical Hebrew: Evidence for an Historical Reading of Genesis 1:1–2:3

1	Production of a text by an author	640
2	3-D plots of paired-texts data, showing the contrasting finite verb distribution for narrative and poetic versions of the same event	653
3	Cluster analysis plot	654
4	3-D bar graph of finite verb distribution in narrative	658
5	3-D bar graph of finite verb distribution in poetry	660

Figure	Title	Page
6	Scatter plot showing the ratio of preterites to finite verbs versus the ratio of imperfects to finite verbs	661
7	Scatter plot showing the ratio of preterites to finite verbs versus the ratio of perfects to finite verbs	661
8	Side-by-side plot of the distribution of the relative frequency of preterites in narrative <i>vis-à-vis</i> poetry	662
9	Logistic regression curve showing the probability a passage is a narrative based on the ratio of preterites to finite verbs	667
10	Plot showing the band of possible logistic curves derived from random samples from the total population of texts	674
A1	3-D bar graph of the finite verb distribution in selected narrative texts	693
A2	3-D bar graph of the finite verb distribution in selected poetic texts	694
A3	Scatter plot for selected texts, with preterites/(finite verbs) versus imperfects/(finite verbs)	696
A4	Scatter plot for selected texts, with preterites/(finite verbs) versus perfects/(finite verbs)	696
C1	Scatter plot with preterites/(finite verbs) versus waw-perfects/(finite verbs), which shows the negative correlation of these verb frequencies in narrative	704

**Summary of Evidence for a Young Earth
from the RATE Project**

1	SEM photomicrograph of a zircon crystal containing ^{238}U , ^{206}Pb , and ^4He extracted from the Jemez granodiorite, Fenton Lake, New Mexico	740
2	Comparison of diffusivity between Creation and uniformitarian models in zircon as a function of temperature	741
3	Photos of ^{210}Po and ^{218}Po radiohalos	744

Figure	Title	Page
4	Plot of radiohalo occurrence in granites versus conventional age for three categories of granites —pre-Flood, Flood and post-Flood (?)	745
5	Composite plot of isochron age versus atomic weight for four radioisotope pairs and four Precambrian formations in Grand Canyon	750
6	Potential energy seen by the α -particle versus distance from the nuclear center	751
7	Histogram of measured $^{14}\text{C}/\text{C}$ in percent of modern carbon concentration for forty Phanerozoic biological samples as reported in the conventional literature	754
8	Side-by-side scatter plot of preterite verb forms in narrative passages versus poetic	758
9	Plot showing the band of possible logistic curves derived from random samples from the total population of texts	759

Prologue

John D. Morris, Ph.D.*

Evolution and deep time go hand in hand. Eons of time are required to generate and accumulate rare beneficial mutations into the vast array of life we see today. Natural selection cannot produce them, it only selects from the various mutants present. As the late George Wald, former Harvard biology professor, has said:

Time is in fact the hero of the plot . . . Given so much time, the “impossible” becomes possible, the possible probable, and the probable virtually certain. One has only to wait: time itself performs the miracles
(The origin of life, *Scientific American*, 191(2), p.49, 1954).

It’s as if time heals all wounds. Time shrouds all the problems of evolution from view. But, what if the eons of time are a myth?

The authors of this book are convinced that evolution does not happen today, did not happen in the past, and could not happen ever. In fact, the more time available, the more deterioration of the genome occurs, and extinction will prevail. In reality, time is the enemy of evolution, not its hero. But without deep time, evolution can’t even be entertained.

Concepts speculating on the long ago past don’t occupy the same tier of credibility as present day observations. The historical sciences may be legitimate exercises, but they are not the same as the science of observable processes.

For instance, we know how a clam lives, assimilates its food, moves around, reproduces and dies. Furthermore, we observe an impressive variety of clams, and in many cases we even know ancestral relationships among some of the varieties, for they developed in observable time. But what non-clam evolved into a clam in the unobserved past? How did it happen? These historical questions can’t be answered with certainty

* *President, Institute for Creation Research, Santee, California*

in the present. How can we investigate the long-ago past?

Geology students are taught to approach a rock outcrop or laboratory experiment with multiple working hypotheses in mind. Predict the data expected from each hypothesis, and then put them to the test. Gather the data. Gather **all** the data. Then see which hypothesis is best supported by the data. That hypothesis is the one most likely correct.

But time questions differ from others. Lacking a time machine, we can't scientifically observe the past. Today we can only observe and test the remnants of past processes preserved in the present. Thus the past, especially the long-ago past, is inaccessible to science. Even so, deep time has achieved immunity from comparison to any other model. To many, the reality of immeasurably long ages has become such a dogma it never gets questioned at all. The investigator may try to fine tune a date—is the rock 1.35 or 1.37 billion years old?—but no totally different hypothesis merits consideration. Until now, that is.

In 1997 an eight year research initiative to investigate this very issue was launched. Entitled **Radioisotopes and the Age of The Earth (RATE)**, and staffed by experts qualified in relevant fields, it attempted to test the validity of radioisotope dating of rocks, source of the main evidence for deep time. In the true spirit of multiple working hypotheses, these scientists determined to put the basic concept to the test. They determined to gather data heretofore ignored or censored by adherence to only one idea. They purposed to run experiments never before conceived. They demanded that the deep time way of thinking be put to the test, and results compared to the expectations of both old and young earth models. They were intent on seeing which of the two schools of thought was more likely correct.

It would be inaccurate to claim that the RATE scientists had no bias. All are dedicated Christians and all hold the Bible as correct in all its teachings, even in matters of science and history. They have become convinced that belief in the Bible is a reasonable position, well supported by facts and logic. While scientists often make pronouncements contrary to Scripture, no verified fact of science contradicts any of its teachings, even as it relates to the unobserved past. The Bible doesn't give all the details, but it does provide the overall framework within

which historical and scientific data can be interpreted in a robust and intellectually satisfying manner.

The concept of biased scientists may come as a surprise to some, but in reality all investigators have a bias before starting their studies and all experiments are chosen and conducted within that bias. One's thinking can be dominated by generally uniform processes over long ages or by rapid and catastrophic processes over a comparatively short timescale. Since all scientists are locked into the present, studying data and running experiments in the present, limited by their present knowledge, skills and logic, accurately reconstructing the past is virtually impossible. Without a guide, without the big picture provided by a capable and reliable observer of the past, we will all fall short of absolute truth. The RATE scientists are convinced that the Bible's picture of the past is the proper one to inform our present investigation.

The Bible tells of an orderly progression of six 24-hour days only thousands of years ago during which all things were created. Each step was necessary before the next until the earth was fully prepared for animal life and finally man. The oceans, the atmosphere, the continents, the plants, the Sun, Moon, and stars, the animals—each formed by creative processes quite unlike processes of today—each in its place and each accomplishing its purpose. Finally, with man as its steward, it was all “very good” (Genesis 1:31) from the Creator's perspective. But man then chose to reject God's authority over him, immediately precipitating the ruination of creation, followed by a world-restructuring flood in Noah's day. Today we live and do our science in the cursed, flooded, remnant of a once “very good” world, making historical investigations difficult.

If we deny the historicity of these great world-changing events, we have little chance of discerning earth's true past. Without the certainty of a fully-functional earth created by God in the beginning, we might misinterpret that functional maturity for age. Without factoring the great Flood into our thinking, we might assign great time spans to things formed very rapidly in that high energy environment. If we limit our thinking to the processes happening today, at only the rates, scales and intensities we observe today, we cannot arrive at the truth about

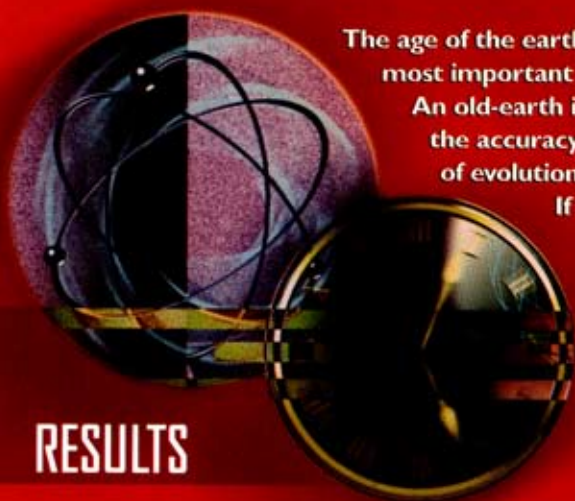
the earth's past and how it came to be in the state it is in today. With the Bible's big picture as our framework, we have a chance of properly reconstructing the earth's history and understanding its present condition.

During the first three years of the RATE initiative radioisotope dating methods and theory were put to the test. The results of those methods were shown to be discordant, inconclusive and sometimes bizarre. Only by selective reporting of the results, and blind adherence to the underlying unprovable assumptions involved, do they even appear to point in the direction of deep time. In short, it was conclusively shown that the radioisotope dating methods do not unequivocally yield the accurate ages of the items tested. But they were doing something. What were they really showing? Is there a better understanding of them which can replace the failed one? The RATE book published after the first three years revealed the questionable state of the radioisotope dating methods and proposed experiments which could shed some light in the darkness.

The next five years were occupied by conducting those experiments and analyzing the data and theory. This book presents the results. Of course, not every question was asked, thus much more remains to be done. But every investigation attempted yielded a positive result for the Creation/Flood/young earth model. Numerous other investigations were suggested.

Does this work prove the young earth model? Of course not, as no historical reconstruction can be fully proved. But it does show that of the two viewpoints the young earth model is better supported and more consistent with **all** the radioisotope evidence.

Thus this book opens a new chapter in the origins controversy. As never before it calls into question the deep time model and places the Biblically compatible young earth model on a level of scholarship never before achieved and archived. Its pages contain many profound thoughts, which will shake current scientific orthodoxy to its core. It deserves careful consideration by all who value truth.



RESULTS

The age of the earth stands out as one of the most important issues among Christians today! An old-earth interpretation clouds our view of the accuracy of Scripture. It supports the theory of evolution. It affects our perception of God.

If Scripture can't be trusted on the age of the earth, how can it be trusted on other issues?

But have we been misled about the reliability of radioactive dating methods? The RATE group believes we have. The RATE group, consisting of eight young-earth creationist geologists, geochemists, geophysicists, physicists, and a Hebraist,

cooperated to research the issue of *Radioisotopes and the Age of the Earth*. They dared to ask the tough questions and thus found an alternative explanation for the billions of years conventionally assigned to rocks. They found answers like:

- Large amounts of nuclear decay have occurred during earth history.
- Helium concentrations in rocks confirm massive nuclear decay.
- Helium diffusion and radiohalos document accelerated nuclear decay.
- Coal and diamonds are young because they contain carbon-14.
- Theoretical studies support accelerated decay.
- Conventional dating methods are unreliable.
- Creation and the Flood are recent historical events.
- The Creation and Flood accounts are accurate historical narratives.

These and many other answers are provided in this book. The RATE researchers have solved a major portion of the radioisotope riddle. This book reports the answers to the questions raised in *Radioisotopes and the Age of the Earth* at the beginning of the five-year research project in 2000. A lay version of this report and a video documentary both entitled *Thousands not Billions: Challenging an Icon of Evolution* are also available.


INSTITUTE
FOR CREATION
RESEARCH


CREATION
RESEARCH
SOCIETY

ISBN: 0-932766-81-1

